SCOPUA Journal of Applied Statistical Research (JASR)

Vol.1, Issue 3, December 2025
DOI: https://doi.org/10.64060/JASR.v1i3.2

An Enhanced Burr Type III Distribution: Simulation Studies and Practical Applications

Manahil Fatima [1], Muzna Sarwar [1*], Shoaib Iqbal [1], Zawar Hussain [1], Farrukh Jamal [2]

[1]Department of Statistics, Faculty of Computing, The Islamia University of Bahawalpur, Pakistan

[2]Department of Statistics, Faculty of Science, University of Tabuk, KSA

* Corresponding Email: muznastatphd@gmail.com

Received: 02 July 2025 / Revised: 01 September 2025 / Accepted: 09 September 2025 / Published online: 17 September 2025

ABSTRACT

In this paper, we introduce a new three-parameter distribution, the New Exponentiated Burr Type III distribution (NEBIII), which is a member of the Generalized (G)-family of continuous distributions. The mathematical features that are derived include the mode, actuarial measures, order statistics, the analytical forms of the density and hazard functions, and explicit formulations for the moment generating function (MGF). The Maximum Likelihood Estimation (MLE) approach is used to estimate the model parameters. A simulated research with different sample sizes is used to evaluate the estimation's efficacy. The versatility and adaptability of the proposed distribution family are demonstrated on four real-world data sets. Additionally, we examine a Mixture of the Exponential and Exponentiated Burr Type III Distributions, identifying various mathematical characteristics and demonstrating their application to actual data.

Keywords*:* NEBIII; MEBE; MLE

1. Introduction

Medical statistics, agricultural statistics, mathematics statistics, reliability analysis, survival analysis, biostatistics, and computational statistics have grown in importance, actuarial statistics has also become more important in statistical study. Real-world phenomena can be predicted and described with the help of statistical distributions. One of the most important statistics problems is deciding which probability distribution should be used to conclude the actual data being studied. Lifetime data can be modeled using a variety of probability models, including exponential, Weibull, Burr XII, Burr III, beta, gamma, log-logistic, and others. Moreover, these conventional models are often inadequate for modeling lifetime data, as noted by [1], highlighting the need for updated versions of existing distributions, as proposed by [2]. Due to their effectiveness in capturing asymmetric and complex random events, these models offer new opportunities for both theoretical and practical researchers to tackle real-world challenges, as discussed by [3].

The statistical literature is full of examples of exponentiated models and their effective use in a variety of applied sciences. The exponentiated-G (Exp-G) class, is also one of the most used generalization methods by [4]. Many researchers use mixture distributions extensively for application, survey estimates, and discussion. Using various methods, several statisticians recently created new, more adaptable Mixture models. In certain cases, the inverse Weibull mixing model with negative weight can be used to represent a system's output, as stated in [5]. As explained in [6], the mixture model of two inverse Weibull distributions was analyzed in terms of hazard rate and graphical representation. Furthermore, [7] looked at the hazard rate, graphs, and statistical properties of a combination of three inverse Weibull distributions.

2. Literature Review

The Burr-III distribution has been extended in recent research to increase its adaptability and usefulness in lifetime data analysis. A three-parameter extended Burr-III distribution was presented by [8], who also looked at its reliability and statistical characteristics. In addition to empirical applications to real datasets, their study includes Monte Carlo simulations to evaluate parameter estimates under various scenarios. The suggested model showed better fit than prior Burr-III extensions. By incorporating various hazard rate shapes and distributional properties, [9] improved the effectiveness of modeling complicated real-world datasets using a modified Burr-III Odds Ratio–G distribution. Similarly, using the logit of the Burr-III random variable, [10] suggest a new family of distributions known as the odd Burr-III family of distributions. [11] introduced two new distributions: the odd Burr III-G power series (OBIII-GPS) class of distributions (CoDs) and its subclass, the odd Burr III-Weibull power series (OBIII-WPS). Applications of the Burr III-Weibull quantile function in reliability analysis were presented by [12]. The Modified Burr-III Distribution Properties, Estimation, Simulation, with Application on Real Data was introduced by [13]. All together, these contributions show how the Burr-III family is being generalised to give statisticians more flexible tools for reliability analysis and real-data applications.

3. Objectives of the study

The following four main goals are the focus of this study.

1. Presenting the exponentiated-G (E-G) family-based Burr–III (B-III) distribution in a more adaptable four-parameter form. The New Burr III Distribution with Mixture of Extended Distribution (NEB-III) is the name of the suggested model. Explicit representations of certain of the (NEB-III) distribution's dependability and statistical characteristics are obtained. The (B-III) model is a specific instance of this distribution.
2. Using the survival mixture approach, a mixture of the NEB-III distribution known as the Mixture of Extended Burr-III (MEB-III) distribution is proposed. The (MEB-III) distribution has a hazard rate shape that decreases.

This study covers the use of traditional estimation methods, such as MLE and log-likelihood, to estimate the parameters of the NEB-III model. The effectiveness of various estimators is assessed and contrasted using the simulation data in order to identify the optimal method for parameter estimation.

3. The empirical significance of the NEB-III and MEB-III distributions is investigated using two real-world data sets. In modelling data, the two introduced models outperform other competing continuous distributions.

There are seven sections in the paper. The new NEB-III distribution is presented in Section 2, and its features are derived in Section 3. We describe the NEB-III distribution's mixture in Section 4. The effectiveness of two methods for calculating the NEB-III parameters is evaluated using simulation data in Section 5. The potential and importance of the new distributions are illustrated in Section 6 by applying them to two real-world data sets. The estimation of NEB-III and MEB-III under the CSALT model is also examined in this part, and the results are verified using real data. Lastly, some closing thoughts are given in Section 7.

4. Motivation of the Study

In life span and reliability modelling, the classical Burr-III (BIII) and Burr-XII (BXII) families are well-established baselines because of their tractable forms and ability to reflect hefty tails. Their typical low-dimensional parameterizations, however, restrict the variety of shapes they may depict: BIII and BXII are unable to separately adjust skewness and tail behavior, and they frequently generate monotone hazard functions. Consequently, these models might offer a less ideal fit for empirical data with non-monotonic hazard rates (such as bathtub or unimodal shapes), significant skewness, or kurtosis that exceeds the capacity of two-parameter models.

In order to overcome these constraints, the suggested three-parameter extended Burr-III distribution offers more shape control while maintaining closed-form representations of its essential characteristics. A wider range of density and hazard rate behaviors, including non-monotonic forms, are made possible by this addition without adding undue complexity. In addition, the model routinely yields better goodness-of-fit findings than BIII, BXII, EBXII, and OBIIILx and performs dependably under maximum likelihood estimation. These benefits show that it has the potential to be a more flexible and successful substitute for modelling intricate lifetime and reliability data.

The strengths of the proposed model — expanded shape flexibility, maintainable analytic tractability, and regular inferential behavior — explain why it can outperform BIII, BXII, EBXII, and OBIIILx in practice. These theoretical arguments are corroborated by the simulation results and empirical comparisons reported in Sections 6, Simulation study of the NEBIII distribution, and 7.1 Applications of the NEBIII distribution, where the proposed model consistently attains lower AIC/BIC

values, superior goodness-of-fit statistics, and more stable parameter estimates across a range of sample sizes and data scenarios.

5. Development of the Exponentiated Burr Type III (NEB-III) Distribution

Several types of cumulative distribution functions for data fitting were suggested in [14]. The Burr distribution system has two common models, the Burr XII (BXII) and BIII. The Burr Type III distribution, also known as the inverse Burr distribution or the Dagum type distribution, is commonly used with type XII in statistical modelling. Thus, it cannot be used to represent lifespan data with a bathtub-shaped hazard function, such as degradation and human mortality, because the shape parameter is essential for determining the hazard rate of the BIII distribution, which may be unimodal as well as decreasing. Numerous generalisations have been proposed to expand the use of the BIII distribution due to its extreme flexibility. The Exponentiated (EBIII) distribution extends the BIII model by adding a second shape parameter. Extending Burr-type models with an exponentiated transformation to increase skewness and hazard shape flexibility provides the theoretical motivation. The EBIII distribution's cumulative distribution function (CDF) is provided as follows,

$$G(x) = (1 + x^{-b})^{-\alpha}, \tag{1}$$

where $\alpha, b, x > 0$.

In this section, we suggest a novel addition to the NEBIII model that will increase its adaptability to modeling different kinds of data in a range of domains. Using the extended CDF supplied by [15], the New Extended Burr-III distribution is created. In addition to being used to enlarge the Topp-Leone family of distributions by [16] and the Kumaraswamy family by [17], this technique was initially employed to develop the Beta generator of distributions.

The NEB-III distribution's PDF and CDF are as follows.

$$F(x) = e^{-[k\log(x^{-b}+1)]^{\theta}}, \qquad x > 0, \tag{2}$$

We assume $k = \alpha\beta$ to avoid the identifiable problem, and k > 0, is the scale parameter and b, θ > 0 are shape parameters. The pdf of NEBIII is obtained from (4), as

$$f(x) = \frac{b\,\theta\,k^{\theta}}{x(1+x^{b})}\,[\log(1 + x^{-c})]^{\theta-1} e^{-[k\log(x^{-b}+1)]^{\theta}}. \tag{3}$$

The cumulative hazard rate function (Hrf), hazard rate function (hrf), inverted hazard rate function (rf), and survival function (SF) are as follows:

$$S(x) = 1 - e^{-[k\log(x^{-b}+1)]^{\theta}}, \tag{4}$$

$$h(x) = \frac{b\,\theta\,k^{\theta}[\log(x^{-b}+1)]^{\theta-1} e^{-[k\log(x^{-b}+1)]^{\theta}}}{x(1+x^{b})\left[1-e^{-[k\log(x^{-b}+1)]^{\theta}}\right]}, \tag{5}$$

$$r(x) = \frac{\frac{b\,\theta\,k^{\theta}}{x(x^{b}+1)}[\log(x^{-b}+1)]^{\theta-1} e^{-[k\log(x^{-b}+1)]^{\theta}}}{e^{-[k\log(x^{-b}+1)]^{\theta}}} \tag{6}$$

$$H(x) = -\log(1 - e^{-[k\log(x^{-b}+1)]^{\theta}}). \tag{7}$$

5.1 The PDF and hrf shapes

We plotted hrf and PDF for the NEB-III distribution with various parameter values to investigate the different distributional behaviors and geometries.

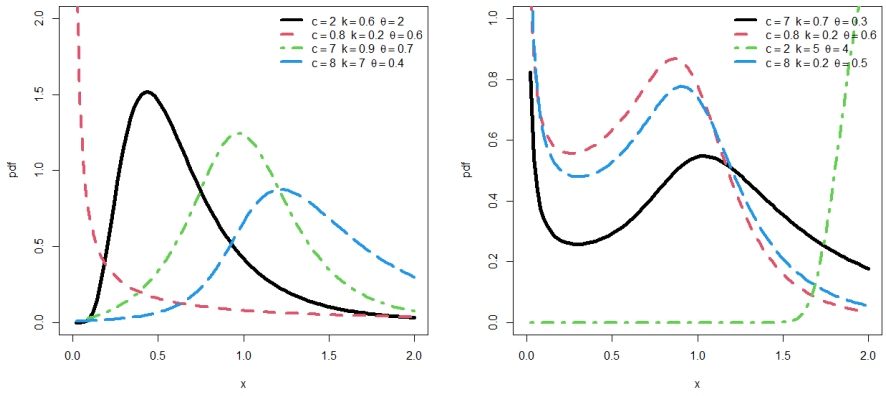

Figure 1: The PDF plot of the NEBIII distribution.

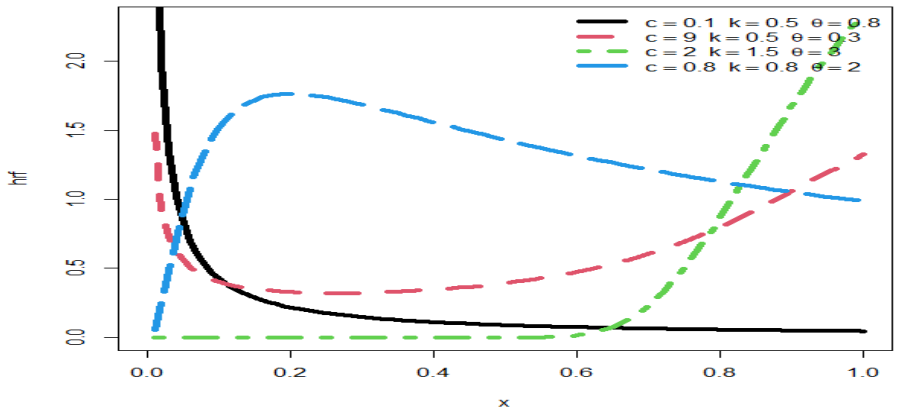

Figure 2: NEBIII distribution's hrf representation.

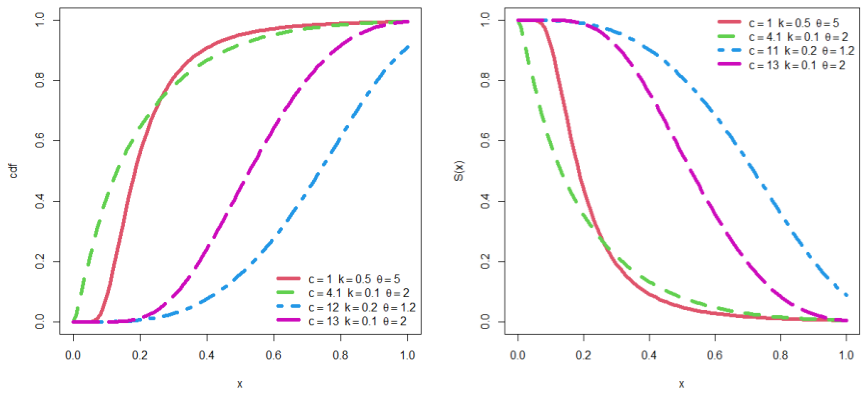

Figure 3: Visualizations of the NEBIII distribution using CDF and SF.

This family can produce a variety of density forms, such as left-skewed, right-skewed, symmetric, decreasing, increasing, and decreasing-increasing-decreasing patterns, as can be seen from the plots in Figures 1 and 2. Hrf shapes include bath-tub, upside-down bathtub, J-shaped, and reverse J-shaped forms. The CDF is a non-decreasing function, while the SF is a decreasing function, as shown in Figure 3.

6 Properties of the NEB-III Distribution

The Quantile Function, Analytical Shape of Density, Analytical Shape of Hazard Rate, Mode, MGF, Rth moments, Mean Deviation from the Mean, Bonferroni Curve, Lorenz Curve, Zenga Index, Atkinson Index, Pietra Index, order statistics, and generalised entropy are among the mathematical properties of NEBIII that we were able to obtain.

6.1 Quantile Function

The quantile function (qf) is important to understand the median and other positional metrics. Furthermore, one essential tool for producing random variates is qf. After inverting equation (4), the qf can be obtained as follows

$$x_q = \left[e^{\left[-\frac{1}{k}(\log(q))\right]^{\frac{1}{\theta}}} - 1 \right]^{-\frac{1}{b}}. \tag{5}$$

6.2 Analytical shape of density

It is feasible to describe the density forms analytically. The analytical shape of density is obtained by using (3),

$$\log f(x) = \log\left[(bk\theta) - \log\,(x(1+x^b)) - \left(k\log\left(x^{-b}+1\right)\right)^{\theta} + (\theta-1)\log\,(k - \log(x^{-b}+1))\right],$$

Taking derivation w.r.t "x"

$$\frac{\partial \log f(x)}{\partial x} = \left[\log(bk\theta) - \log\left[x\left(1+x^b\right)\right] - \left(k\log\left(x^{-b}+1\right)\right)^{\theta} + (\theta-1)\log(k\log\left(x^{-b}+1\right))\right],$$

$$\frac{bkx^{-b-1}\theta\left(k\log\left(x^{-b}+1\right)\right)^{\theta-1}}{x^{-b}+1} - \frac{cx^{-b-1}(\theta-1)}{(1+x^{-b}\log(1+x^{-b}))} - \frac{1+x^b+bx^b}{x(1+x^b)} = 0.$$

6.3 Analytical shape of hazard rate

It is feasible to describe the hazard rate forms analytically. The analytical shape of the hazard rate is obtained by using (4),

$$\log \mathrm{h}(x) = \log\left[(bk\theta) + (\theta-1)\log\left[k\log\left(x^{-b}+1\right)\right] - \log\left[e^{k\log\left(1+x^{-b}\right)^{\theta}} - 1\right]x(1+x^b)\right],$$

Taking derivation w.r.t "x"

$$\frac{\partial \log h(x)}{\partial x} = \frac{bx^{-b-1}(\theta-1)}{(1+x^{-b})\log(1+x^{-b})} - \left[b\left(e^{\left(k\log\left(1+x^{-b}\right)\right)\theta}\right)\right]x^b + \left[e^{\left(k\log\left(1+x^{-b}\right)\right)^{\theta}} - 1\right]\left(1+x^b\right)$$

$$- \frac{be^{\left(k\log\left(1+x^{-b}\right)\right)^{\theta}} kx^{-b}\left(1+x^b\right)\theta\left(k\log\left(1+x^{-b}\right)\right)^{\theta-1}}{1+x^{-b}}\left[\left(e^{\left(klog\left(1+x^{-b}\right)\right)^{\theta}} - 1\right)x\left(1+x^b\right)\right] = 0.$$

6.4 Expansions and approximations

Some distributional characteristics can be more efficiently computed by utilizing the series representation of a PDF. The following finding examines this factor for the exponentiated PDF of the NEBIII distribution. (x) can be stated as

$$f\left(x\right) = \sum_{i=0}^{\infty} \varphi_i \Psi\left(x;b,k,\theta\right),$$

where,

$$\varphi_i = \frac{bk\theta\left(-1\right)^i}{i!},$$

$$\Psi\left(x;b,k,\theta\right) = \frac{\left[-k\log\left(1+x^{-b}\right)\right]^{\theta i+\theta-1}}{x^{b+1}\left(1+x^{-b}\right)}.$$

By applying the exponential series expansion, we obtain,

$$f\left(x\right) = \frac{b\theta k e^{-\left(-k\log\left(1+x^{-b}\right)\right)^{\theta}}\left[-k\log\left(1+x^{-b}\right)\right]^{\theta-1}}{x^{b+1}\left(1+x^{-b}\right)},$$

$$= \frac{c\theta k\sum_{i=0}^{\infty}\frac{\left(-1\right)^i}{i!}\left[-k\log\left(1+x^{-b}\right)\right]^{\theta i+\theta-1}}{x^{b+1}\left(1+x^{-b}\right)}$$

$$= \sum_{i=0}^{\infty}\varphi_i\Psi\left(x;b,k,\theta\right) \tag{6}$$

6.5 The Moment generating function of the NEBIII distribution

By using (3), we have the moment generating function of the NEBIII distribution as,

$$M_x(t) = E\left(e^{tx}\right) = \int_0^{\infty} e^{tx} \frac{bk\theta e^{-\left[-k\log\left(1+x^{-b}\right)\right]^{\theta}} \left[-k\log\left(1+x^{-b}\right)\right]^{\theta-1}}{x^{b+1}\left(1+x^{-b}\right)} dx,$$

By utilizing a weight function w_i and Gamma function $(\cdot)$, we can further simplify the expression of $E\left(e^{tx}\right)$ as follows,

$$E\left(e^{tx}\right) = \sum_{i=0}^{\infty} v_i \Gamma\left(\theta i + \theta\right)$$

Where, the series v_i is defined as,

$$v_i = \theta \sum_{j=0}^{\infty} \sum_{l=0}^{\infty} \frac{(-1)^{i+j+\frac{r}{b}}}{l!i!} \binom{-\frac{r}{b}}{j} \left(\frac{j}{k}\right)^{-(\theta i+\theta)}$$

6.6 The NEBIII distribution's r^{th} moment

The r^{th} moments expression for NEBIII is given by using (3), as

$$E\left(x^r\right) = \int_0^{\infty} \frac{x^r bk\theta e^{-\left[-k\log\left(1+x^{-b}\right)\right]^{\theta}} \left[-k\log\left(1+x^{-b}\right)\right]^{\theta-1}}{x^{b+1}\left(1+x^{-b}\right)} dx,$$

Finally, we have, Utilising a weight function w_i and the Gamma function $(\cdot)$, we can further simplify the expression of m_r as follows,

$$m_r = \sum_{i=0}^{\infty} w_i \Gamma\left(\theta i + \theta\right), \tag{7}$$

where the series wi is defined as,

$$w_i = \theta \sum_{j=0}^{\infty} \frac{(-1)^{i+j+\frac{r}{b}}}{i!} \binom{-\frac{r}{b}}{j} \left(\frac{j}{k}\right)^{-(\theta i+\theta)}, \tag{8}$$

and $\frac{r}{b} > 0$ is a real number.

The first moment of the series (X) is obtained as:

Using eq (7) and eq (8), put r=1 then we get the first raw of NEBIII is define as

$$E\left(X\right) = \mu = \sum_{i=0}^{\infty} \varphi_i \mu_i \quad . \tag{9}$$

6.7 rth incomplete moment

It is possible to represent and approximate the rth incomplete moment as

$$m_r(t) = E\left(X \le t\right) = \int_0^t x^r f\left(x\right) dx = \sum_{i=0}^{\infty} \varphi_i \int_0^t x^r \Psi\left(x; b, k, \theta\right) dx,$$

By describing this incomplete moment in terms of an incomplete Gamma function $(\cdot)$ and a weight function (t), it can be further simplified,

$$m_r(t) = \sum_{i=0}^{\infty} w_i(t) \gamma\left(\theta i + \theta, \frac{j}{k} y\right), \tag{10}$$

Where, the series wi and y are defined as,

$$w_i = \theta\sum_{j=0}^{\infty}\frac{(-1)^{i+j+\frac{r}{b}}}{i!}\binom{-\frac{r}{b}}{j}\left(\frac{j}{k}\right)^{-(\theta i+\theta)}, y = -k\log\left(1+x^{-b}\right),$$

6.8 Mean deviation from the NEBIII distribution mean

The sum of the departures from the mean is a measure of the degree of scatter in the population. The following defines the mean deviation from the mean:

$$\delta_1(x) = 2\left[\mu F(\mu) + \int_0^x xf(x)dx\right],$$

Using the eq (2) and eq (10), mean deviation from mean is written as,

$$\delta_1(x) = 2\left[\mu e^{-\left[-k\log\left(1+\mu^{-b}\right)\right]^{\theta}} - w_i(t)\gamma\left(\theta i+\theta, \frac{j}{k}y\right)\right]. \quad (11)$$

6.9 The Lorenz curve of the NEBIII distribution

A measure was proposed in [18]. The graph of the ratio against F(x) with the characteristics L(p) ≤ p, L(0) = 0, and L(1) = 1 is referred to as the Lorenz curve for a positive random variable X. L(p) is the percentage of total income that goes to those with the 100% lowest earnings, assuming X is the annual income. L (p) = p for all p if everyone makes the same amount of money. One way to think of the area between the Lorenz curve and the line L (p) = p is as a measure of income inequality, or more broadly, of X's variability. For the NEBIII distribution, it is widely recognized that the Lorenz curve is defined by,

$$L = \frac{1}{\mu}\int_0^x xf(x)dx = \frac{1}{\mu}\sum_{i=0}^{\infty} w_i(t)\gamma\left(\theta i+\theta, \frac{j}{k}y\right). \quad (12)$$

6.10 The Bonferroni Curve of the NEBIII Distribution

A measure of income inequality based on partial means was intended by [19], which is preferable when the existence of units with incomes much lower than others is the primary cause of income inequality. The relationship can be used to calculate the Bonferroni Curve, Using (12) and (2), we get,

$$B = \frac{L}{F(x)} = \frac{1}{\mu e^{-\left[-k\log\left(1+x^{-b}\right)\right]^{\theta}}}\sum_{i=0}^{\infty} w_i(t)\gamma\left(\theta i+\theta, \frac{j}{k}y\right)$$

6.11 The Zenga Index of the NEBIII distribution

The following income inequality indicator was first presented by [20].

$$Z = 1 - \frac{\mu_x^-}{\mu_x^+} \quad (13)$$

Using Eq (2) and Eq (10) we obtain,

$$\mu_x^- = \frac{1}{F(x)}\int_0^x xf(x)dx = \frac{1}{e^{-\left[-k\log\left(1+x^{-b}\right)\right]^{\theta}}}\sum_{i=0}^{\infty} w_i(t)\gamma\left(\theta i+\theta, \frac{j}{k}y\right),$$

μ_x^+ define as $= \frac{1}{1-F(x)}\left(\mu - \int_0^x xf(x)dx\right) = \frac{1}{1-e^{-\left[-k\log\left(1+x^{-b}\right)\right]^{\theta}}}\left(\mu - \sum_{i=0}^{\infty} w_i(t)\gamma\left(\theta i+\theta, \frac{j}{k}y\right)\right),$

We obtain the outcome we want by changing the value of μ_x^+ and μ_x^- in Eq 13.

6.12 The Pietra Index of the NEBIII distribution

The Schutz index, also called half the relative mean deviation, was introduced by the [21]. It is described as follows,

$$P_X = \frac{\delta_1(x)}{2\mu},$$

by using (12) we can obtain as,

$$P_X = \frac{1}{\mu}\left[\mu e^{-\left[-k\log\left(1+\mu^{-b}\right)\right]^{\theta}} - w_i(t)\gamma\left(\theta i+\theta, \frac{j}{k}y\right)\right].$$

6.13 Entropy

Entropy measures how unreliable or unpredictable a system is in statistical thermodynamics and information theory. In this context, the NEBIII distribution's Rényi entropy is discussed, which may be calculated with the formula below,

$$R(\rho) = \frac{1}{1-\rho}\log\left[Ef(x)^{\rho}\right],$$

Where $\rho \neq 0$ and $\rho > 0$. An approximation of the expectation term would be:

$$E\left[f(x)^{\rho}\right] = \int_0^{\infty} f(x)^{\rho} dx.$$

The computation, which involves approximating the PDF of the NEBIII distribution raised to a power after replacing these numerical values, is analytically challenging because to the intricacy of the integral. This assumption is approximately met by numerical integration techniques such as Monte Carlo simulation and Gaussian quadrature.

The Rényi entropy becomes the Shannon entropy if $\rho \to 1$, another uncertainty Shannon entropy measure is defined by $E[-\log f(X)]$.

6.14 The Order statistics of the NEBIII distribution

Order statistics are necessary for both theoretical study and real-world applications, especially when looking at a specific sample size, maximum, minimum, and range. Records and details about the operation of order are accessible by [22]. Order statistics are widely employed in many domains, including dependability, quality control, wireless communication, signal processing, classification analysis, survival analysis, and life testing by [23].

The following is the PDF of the rth order statistics of a random sample of size n for the NEBIII distribution,

$$f_{r:n}(x) = \frac{n!}{r!(n-r)!}\left[F(x)\right]^{r}\left[1-F(x)\right]^{n-r} f(x),$$

The following PDF can be generated by inserting Equations (2) and (3) into this equation:

$$f_{r:n}(x) = \frac{n!bk\theta}{r!(n-r)!}\sum_{i=0}^{n-r}\sum_{j=0}^{\infty}\frac{(-1)^{i+j}(r+i)^{j}}{(j!)x^{b+1}\left(1+x^{-b}\right)}\left[-k\log\left(1+x^{-b}\right)\right]^{\theta j+\theta-1},$$

Thus, for the NEBIII distribution, the pdf of minimum order statistics is,

$$f_{1:n}(x) = \frac{n!bk\theta}{(n-1)!}\sum_{i=0}^{n-1}\sum_{j=0}^{\infty}\frac{(-1)^{i+j}(1+i)^{j}}{(j!)x^{b+1}\left(1+x^{-b}\right)}\left[-k\log\left(1+x^{-b}\right)\right]^{\theta j+\theta-1},$$

The NEBIII distribution's maximum order statistics pdf is as follows,

$$f_{n:n}(x) = \frac{n!bk\theta}{(n-1)!}\sum_{j=0}^{\infty}\frac{(-1)^{j}(r)^{j}}{(j!)x^{b+1}\left(1+x^{-b}\right)}\left[-k\log\left(1+x^{-b}\right)\right]^{\theta j+\theta-1}.$$

6.16 MLE of the NEBIII Distribution

We appreciate the reviewer's wise observation regarding the inclusion of other inferential techniques like MPS estimation and Bayesian inference. We completely concur that these methods could improve the research. However, we have limited our study to maximum likelihood estimation (MLE) in order to preserve clarity and prevent the paper from becoming unduly lengthy. MLE's exclusive usage in this study is justified by the literature's widespread recognition of its effectiveness and suitability for creating new probability distributions.

We propose estimating the unknown parameters of the new distribution using the ML method.

Taking log-likelihood function for Eq (3),

$$= \sum_{i=1}^{n} nlog[bk\theta] - \log\left[x\left(1+x^{b}\right)\right] + (\theta-1)\sum_{i=1}^{n}\log\left[klog\left(1+x^{-b}\right)\right] - \sum_{i=1}^{n}\left[klog\left(1+x^{-b}\right)\right]^{\theta}, \quad (14)$$

Differentiate (14) with respect to b, we have

$$= \frac{-\log(x)x^{b}}{1+x^{b}} - (\theta-1)\sum_{i=0}^{n}\frac{\log(x)x^{-b}}{\log(1+x^{-b})(1+x^{-b})} + \sum_{i=0}^{n}\frac{k\theta log x\left[klog\left(1+x^{-b}\right)\right]^{\theta-1}}{1+x^{-b}}.$$

Differentiate (14) with respect to k, we have

$$= \frac{(1+n)(\theta-1)}{k} - \sum_{i=0}^{n}\theta\log\left(1+x^{-b}\right)\left[klog\left(1+x^{-b}\right)\right]^{\theta-1}.$$

Differentiate (14) with respect to θ, we have

$$= \sum_{i=0}^{n}\log\left[klog\left(1+x^{-b}\right)\right] - \sum_{i=0}^{n}\log\left[klog\left(1+x^{-b}\right)\right]\left[klog\left(1+x^{-b}\right)\right]^{\theta}.$$

Table 1: Moments, Kurtosis, and Skewness of X for particular values of the NEBIII parameters (b, k, θ).

$\mu_k^{/}$	NEBIII (2,2,6)	NEBIII (1, 3,5)	NEBIII (4,5,6)	NEBIII (4,2,7)	NEBIII (2,6,8)
$\mu_1^{/}$	1.3271	3.0181	1.4986	1.1441	2.4498
$\mu_2^{/}$	1.7960	10.3016	2.2540	1.3135	6.0509
$\mu_3^{/}$	2.4868	42.9274	3.4031	1.5134	15.0824
$\mu_4^{/}$	3.5379	273.4831	5.1593	1.7503	37.9807
Variance	0.0348	1.1924	0.0080	0.0044	0.0493
S.D	0.1867	1.0919	0.0898	0.0663	0.2220
Skewness	1.6493	3.5615	1.3528	1.2049	1.5423
Kurtosis	15309.6	398.9066	464291.6	529237.7	88836.78
CV	0.1407	0.3618	0.0599	0.0580	0.0906

6.16 Actuarial measures

The probability of a risk event happening is estimated statistically by an actuarial metric. Actuaries assist businesses and organizations in making decisions regarding lending, investments, and risk by using actuarial measurements.

Value-at-Risk

Value-at-Risk, or VaR, is a frequently used statistic to evaluate final market risk. Quantile risk is another term for it, or simply "VaR." Government regulations, commodity pricing, and the volatility of both domestic and foreign markets can all have a big impact on a company's profitability, which makes them crucial for many business decisions. The loss portfolio's value is represented as a percentage. The definition of the NEB-III model is as follows:

$$VaR(q) = \left[e^{\left[-\frac{1}{k}(\log(q))\right]^{\frac{1}{\theta}}} - 1\right]^{-\frac{1}{b}}. \tag{15}$$

Expected Shortfall

Introduced by [24], the expected shortfall (ES) is another crucial financial risk metric that is typically thought to be superior to value at risk. It is specified through the following expression,

$$ES_{q}(x) = \frac{1}{q}\int_{0}^{q} VaR(x)dx \tag{16}$$

For 0 < q < 1, using eq (9) in eq (10).

Tail value at risk

One of the most essential aspects of risk management is risk quantification. From the viewpoints of finance and insurance, tail value at risk (TVaR), sometimes referred to as tail conditional expectation or conditional tail expectation, is an important statistic. If the loss is greater than the VaR, it is defined as the expected value of the loss.

By using Eq 10,

$$TVaR_{q}(x) = \frac{1}{1-q}\int_{VaR_{q}}^{\infty} xf(x)dx = \frac{1}{1-q}\left(\mu - \int_{0}^{VaR_{q}} xf(x)dx\right), \tag{17}$$

Under Let Y ~ NEBIII (c,k,θ) for 0 < V < 1, the tail value at risk (TVaR) is obtained by applying Eq (3) in eq (15).

$$TVaR_{q}(x) = \frac{1}{1-q}\int_{VaR_{q}}^{\infty} xf(x)dx = \frac{1}{1-q}\left(\mu - \sum_{i=0}^{\infty} w_{i}(t)\gamma\left(\theta i + \theta, \frac{j}{k}y\right)\right),$$

Where the series wi and y are defined as,

$$w_i = \theta\sum_{j=0}^{\infty}\frac{(-1)^{i+j+\frac{1}{c}}}{i!}\binom{-\frac{1}{c}}{j}\left(\frac{j}{k}\right)^{-(\theta i+\theta)}, y = -k\log\left(1+VaR_q\right).$$

Tail variance

Tail variance (TV), another significant risk measure, takes into consideration the risk's fluctuation at the tail of the distribution and is explained as follows,

$$TV_q\left(x\right) = E\left(X^2 \mid X > x_q\right) - \left[TVaR_q\left(x\right)\right]^2, \tag{18}$$

$$\text{Let } I = E\left(X^2 \mid X > x_q\right) = \frac{1}{1-q}\int_{VaR_q}^{\infty} x^2 f\left(x\right)dx = \frac{1}{1-q}\left(\mu - \sum_{i=0}^{\infty} w_{2i}\left(t\right)\gamma\left(\theta i+\theta, \frac{j}{k}y\right)\right),$$

Where the series *wi* and y are defined as,

$$w_{2i} = \theta\sum_{j=0}^{\infty}\frac{(-1)^{i+j+\frac{2}{c}}}{i!}\binom{-\frac{2}{c}}{j}\left(\frac{j}{k}\right)^{-(\theta i+\theta)}.$$

Tail variance premium (TVP)

TVP is an additional curial risk metric that combines central tendency and dispersion statistics to more accurately assess the variability of loss along the right tail. When it comes to risk that exceeds a particular threshold, TVP may be an alternate risk measure,

$$TVP_q\left(X\right) = TVaR_q + \delta TV_q \tag{19}$$

The TVP of the NEBIII model is calculated by initially utilizing the formulas in Equations (17) and (18). These intermediate results are then substituted into Equation (19) to obtain the final result of the TVP, where $0 < \delta < 1$.

7. An NEXIII mixture with an exponential (E) distribution (MEBE)

Two distributions combined can be defined as

$$f(x) = p\, f_1(x) \ + (1-p)f_2(x)\,, \tag{20}$$

Here, we presented the cdf and pdf of a "MEBE"—a combination of the EBIII and E distributions.

Let $F_1(x)$ and $f_1(x)$ be the cdf and pdf of EBIII distribution.

$$F_1(x) = e^{-\left[k\log\left(1+x^{-b}\right)\right]^{\theta}}, \tag{21}$$

$$f_1(x) = \frac{b\ \theta\ k^{\theta}}{x\left(1+x^{b}\right)}\left[\log\left(1+x^{-b}\right)\right]^{\theta-1} e^{-\left[k\log\left(1+x^{-b}\right)\right]^{\theta}}. \tag{22}$$

And, $F_2(x)$ and $f_2(x)$ are the CDF and PDF of exponential distribution

$$F_2(x) = 1 - e^{-\mu x}, \tag{23}$$

$$f_2(x) = \mu e^{-\mu x}. \tag{24}$$

Using (22) and (24) in (20), we obtained the pdf of MEBE as

$$f(x) = p\,\frac{b\ \theta\ k^{\theta}}{x\left(1+x^{b}\right)}\left[\log\left(1+x^{-b}\right)\right]^{\theta-1} e^{-\left[k\log\left(1+x^{-b}\right)\right]^{\theta}} + (1-p)\mu e^{-\mu x}, \tag{25}$$

From (21) and (23), we obtained the cdf of MEBE as

$$F(x) = pe^{-\left[k\log\left(1+x^{-b}\right)\right]^{\theta}} + (1-p)(1-e^{-\mu x}). \tag{26}$$

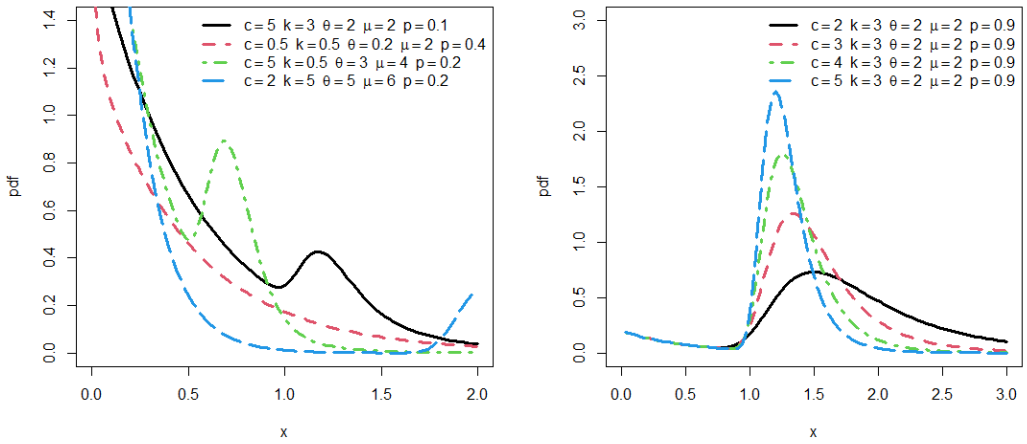

Figure 4: PDF Plots of MEBE for several parametric values.

Figures 4 and 5 display the various shapes of the density, such as symmetric, left-skewed, right-skewed, decreasing, and decreasing-increasing-decreasing distributions.

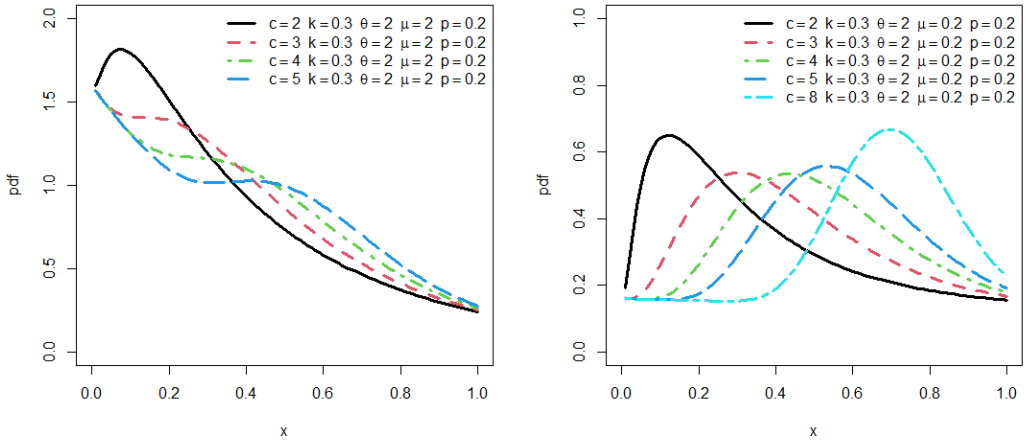

Figure 5: PDF Plots of MEBE for several parametric values.

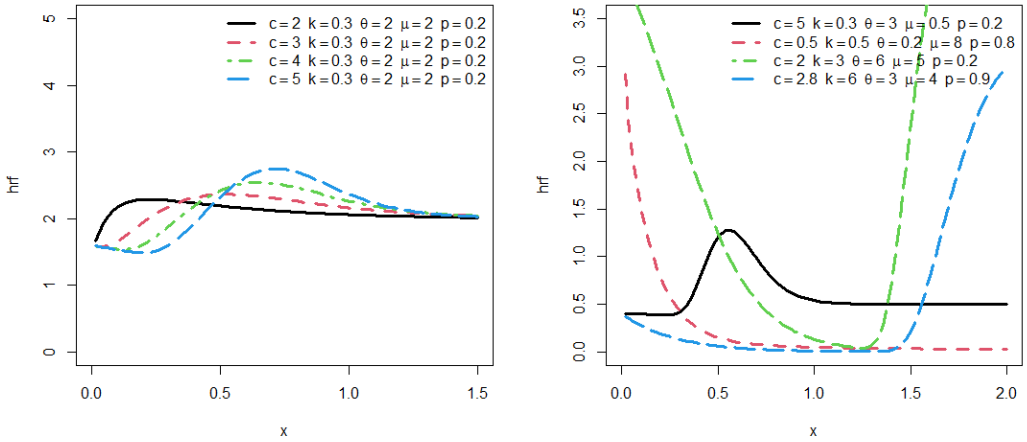

Figure 6: hrf Plots of MEBE for several parametric values.

Figure 6 displays the several HRF shapes, including the J-shaped, bathtub, reverse J-shaped, and upside-down bathtub patterns.

We obtain the SF as follows from (26),

$$S(x) = 1 - pe^{-\left[k\log\left(1+x^{-b}\right)\right]^{\theta}} - (1-\mathrm{p})\lambda(1-\mathrm{e}^{-\lambda x}) \ . \tag{27}$$

From equations (25) and (26), hrf is derived as follows:

$$h(x) = \frac{\frac{pb\,\theta\,k^{\theta}}{x\left(1+x^{b}\right)}\left[\log\left(1+x^{-b}\right)\right]^{\theta-1} e^{-\left[k\log\left(1+x^{-b}\right)\right]^{\theta}} + (1-p)\mathrm{e}^{-\lambda x}}{1-pe^{-\left[k\log\left(1+x^{-b}\right)\right]^{\theta}} - (1-\mathrm{p})\lambda(1-\mathrm{e}^{-\lambda x})} \ . \tag{28}$$

From (28), the reversed hazard rate function is obtained as,

$$r(x) = \frac{\frac{pb\,\theta\,k^{\theta}}{x\left(1+x^{b}\right)}\left[\log\left(1+x^{-b}\right)\right]^{\theta-1} e^{-\left[k\log\left(1+x^{-b}\right)\right]^{\theta}} + (1-p)\mathrm{e}^{-\lambda x}}{pe^{-\left[k\log\left(1+x^{-b}\right)\right]^{\theta}} + (1-\mathrm{p})\lambda(1-\mathrm{e}^{-\lambda x})}.$$

The Hrf is defined as,

$$H(x) = -logS(x),$$

from (17), we get

$$H(x) = -\log(1 - pe^{-\left[k\log\left(1+x^{-b}\right)\right]^{\theta}} - (1-\mathrm{p})\lambda(1-\mathrm{e}^{-\lambda x})).$$

8. Simulation study of the NEBIII distribution

An essential instrument in statistics is simulation analysis, which is used to assess how well estimates work at different sample sizes over partial replication. Therefore, the main focus of this part is the performance parameter estimations of the suggested EBIII model, which is based on simulation study. There are 1000 replications of a simulation process, with various sample sizes (n = 25, 50, 100, and 500). The results of the simulation research showed that as sample size increased, bias, MSE, and average width (AW) of the parameter confidence interval decreased. Conversely, coverage probabilities (CPs) approach the 95% nominal level.

$$\text{MSE}\ (\hat{\vartheta}) = \sum_{j=1}^{1000} \frac{\left(\hat{\vartheta}-\vartheta\right)^2}{1000}, \quad \text{and} \quad \text{Bias}(\hat{\vartheta}) = \sum_{j=1}^{1000} \frac{\hat{\vartheta}}{1000} - \vartheta$$

Table 2: MSEs, AWs, CPs, and Biases for many scenarios.

Scenarios-I (c = 0.5, k = 0.9, theta = 1)						
N	Bais	MSE	CP	LO.bound	UPP.bound	AW
50	-0.022	0.047	0.922	0.138	0.868	0.781
	.052	0.031	0.930	0.617	1.287	0.670
	0.374	1.346	0.962	1.158	3.338	3.927
100	-0.035	0.019	0.944	0.226	0.748	0.525
	0.032	0.015	0.932	0.708	1.156	0.449
	0.126	0.178	0.964	0.588	1.749	1.246
500	-0.056	0.003	0.944	0.386	0.613	0.226
	0.002	0.003	0.960	0.806	0.999	0.193
	0.013	0.010	0.972	0.822	1.204	0.382
Scenarios-II (c = 0.1, k = 0.3, theta = 0.75)						
50	0.006	0.002	0.948	0.037	0.174	0.137
	-0.062	0.009	0.774	0.099	0.378	0.279
	0.296	0.115	0.612	0.733	1.359	0.626
100	0.003	0.001	0.946	0.057	0.148	0.091
	-0.070	0.007	0.648	0.136	0.325	0.189
	0.272	0.085	0.214	0.813	1.230	0.417
500	0.001	0.001	0.956	0.081	0.120	0.039
	-0.073	0.006	0.112	0.185	0.268	0.083
	0.256	0.068	0.034	0.916	1.097	0.181

Table 3: MSEs, AWs, CPs, and Biases for many scenarios.

Scenarios-III (c = 0.3, k = 0.7, theta = 0.2)						
N	Bais	MSE	CP	LO.bound	UPP.bound	AW

50	0.217	0.738	0.912	4.261	5.264	9.494
	-0.548	0.309	0.022	0.032	0.311	0.320
	0.874	0.836	0.004	0.662	1.522	0.895
100	0.067	0.055	0.938	0.101	0.668	0.601
	-0.558	0.315	0.010	0.044	0.240	0.197
	0.830	0.712	0.001	0.760	1.300	0.539
500	0.028	0.010	0.952	0.158	0.497	0.338
	-0.561	0.317	0.009	0.071	0.207	0.136
	0.814	0.671	0.056	0.829	1.199	0.370
Scenarios-IV (c = 0.03, k = 0.9, theta = 0.5)						
50	0.007	0.680	0.978	0.016	0.058	0.042
	-0.504	0.261	0.006	0.209	0.583	0.374
	0.409	0.184	0.126	0.600	1.219	0.619
100	0.003	0.432	0.970	0.020	0.047	0.027
	-0.479	0.234	0.003	0.282	0.560	0.278
	0.456	0.220	0.002	0.717	1.196	0.479
500	0.001	0.203	0.966	0.024	0.036	0.011
	-0.447	0.201	0.002	0.387	0.519	0.132
	0.506	0.259	0.001	0.887	1.125	0.238

9. Applications

Real data sets are used to demonstrate the applicability of EBIII distribution and MEBE distribution.

9.1 Applications of the NEBIII distribution

In this section, we compare the NEBIII distribution with the Burr Type III (BIII), Burr Type XII (BXII), Exponentiated Burr Type XII (EBXII), and Odd Burr Type III Lomax (OBIIILx) distributions. The validity of the fitted models is assessed for each data set using the Kolmogorov-Smirnov goodness-of-fit test. In all cases, the p-values indicate that the models fit the data exceptionally well. To highlight the significance of the EBIII distribution, we present four applications using real data sets in this subsection. In addition to higher p-values for the Kolmogorov-Smirnov test, other statistics such as the Akaike Information Criterion (AIC), Anderson-Darling (A), Cramér-von Mises (W), and p-values indicate a good fit when their values are lower. The necessary computations are performed using the R programming language.

A novel generalization of the Burr Type III distribution that can fit a wider range of real-world datasets than existing models is provided by the proposed CDF, which was motivated by the need for a distribution that can flexibly capture diverse data patterns. The Burr Type III distribution offers a strong baseline because of its heavy-tailed behavior, but its flexibility is limited. Through the use of an exponentiation transformation, we introduce an additional parameter that improves skewness, tail thickness, and hazard rate adaptability.

We used this transformation on four real-world datasets: Failure Time Dataset I, Failure Time Dataset II, a dataset of head and neck cancer (Dataset III), and a dataset of 128 patients with bladder cancer (Dataset IV).

The BFGH (B) method provides the optimal value, while the SAAN (S) method, a global optimisation technique known as simulated annealing, is used to determine the starting value, also referred to as the initial kick. One approach to examine the shape of the hazard function is by using the Total Time on Test (TTT) plot. For a given data set, a convex shape indicates a decreasing hazard, while a concave shape suggests an increasing hazard. A straight diagonal line corresponds to a constant hazard. The TTT plots in Figures 7 and 8 reveal that the data sets exhibit an increasing hazard rate curve, Figures 9 and 10 show that the data sets exhibit an increasing-decreasing-increasing hazard rate curve.

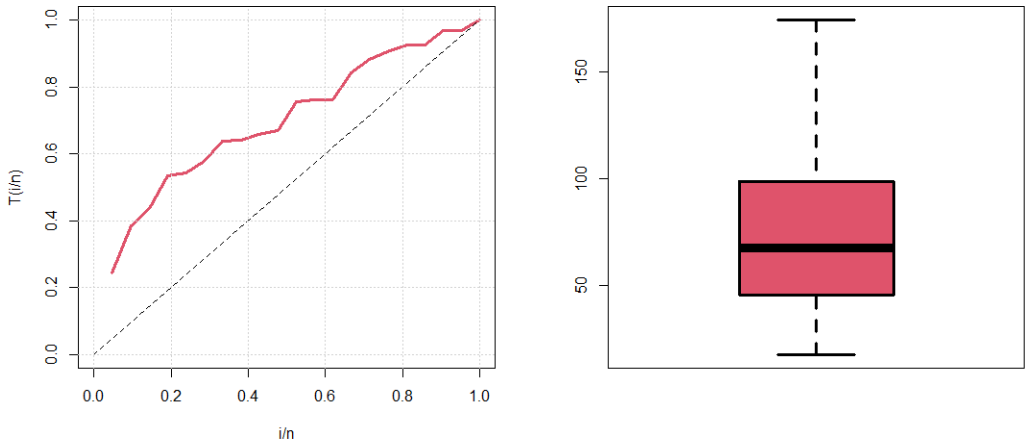

Figure 7: TTT plot and Box plot for the data set 1.

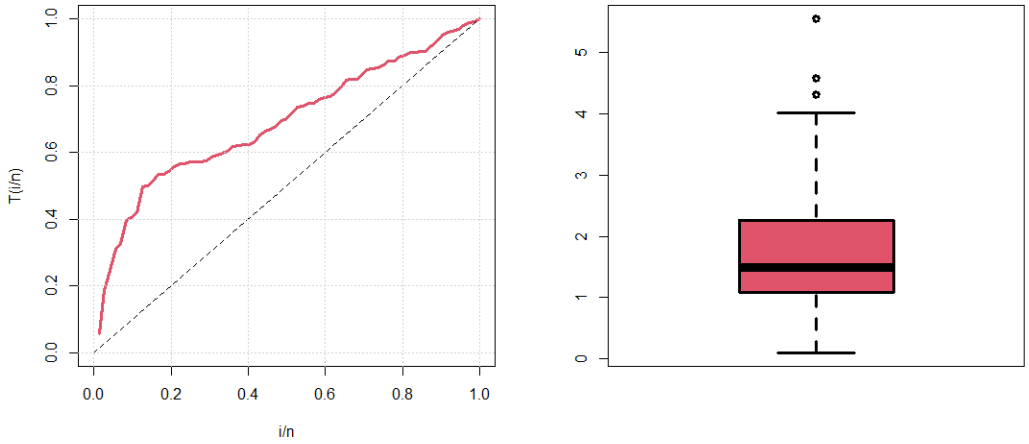

Figure 8: Box plots and TTT for the II data set.

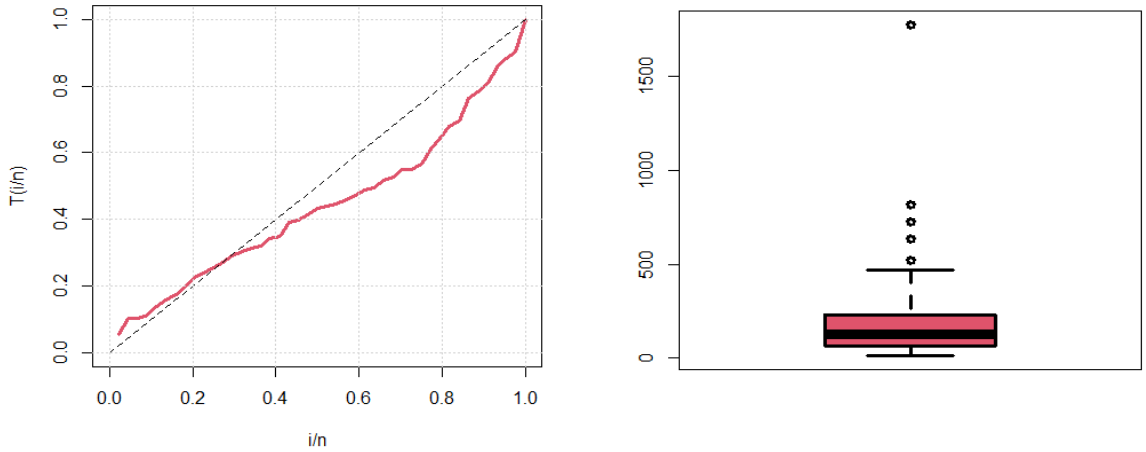

Figure 9: TTT and Box plots for the III data set.

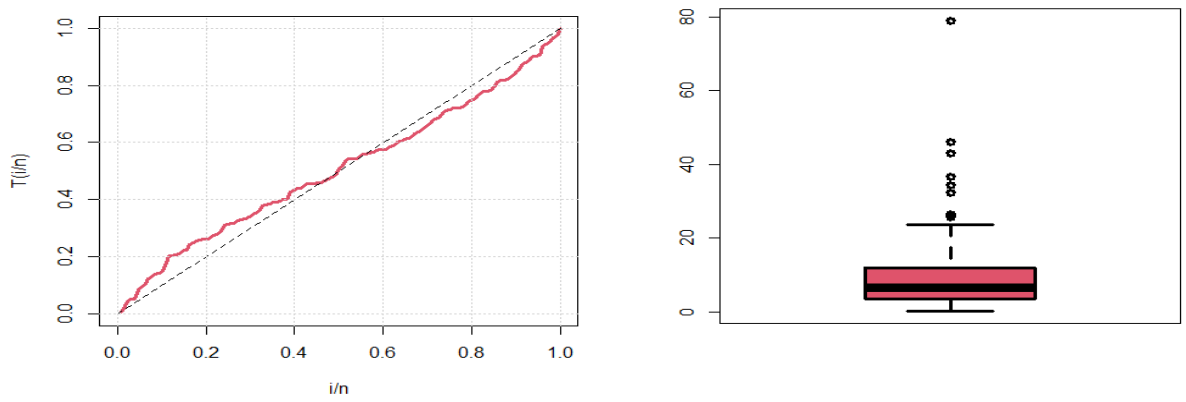

Figure 10: Box plots and TTT for the IV data set.

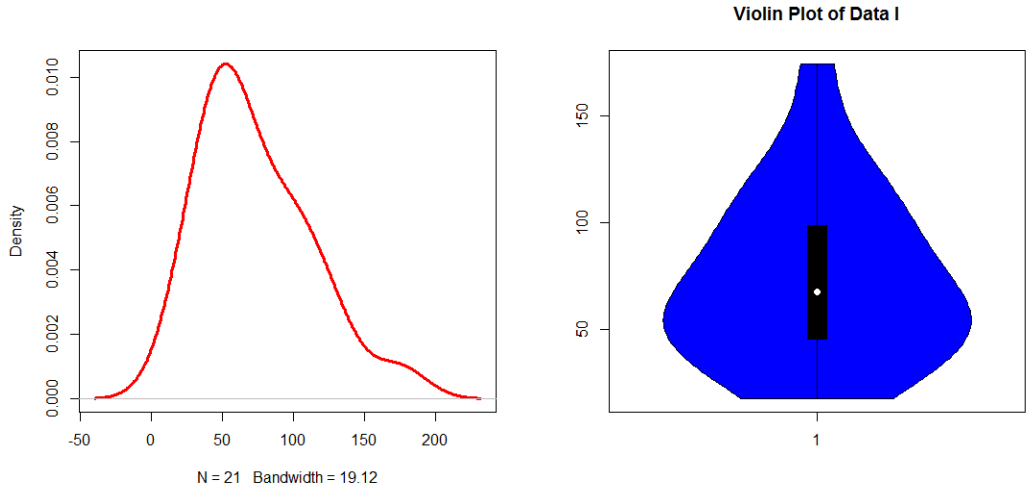

Figure 11: Kernel density plot and violin plot for the Ist data set.

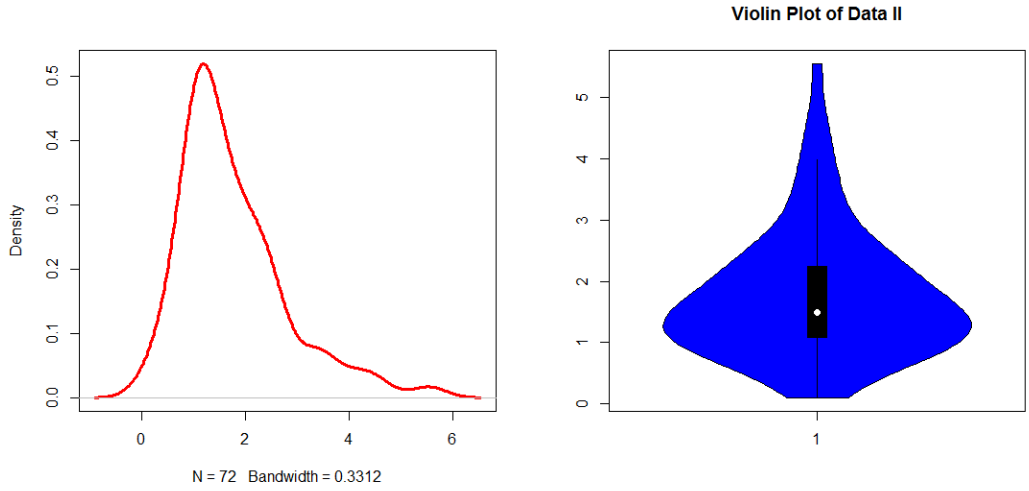

Figure 12: Kernal density and violin plot for the II data set.

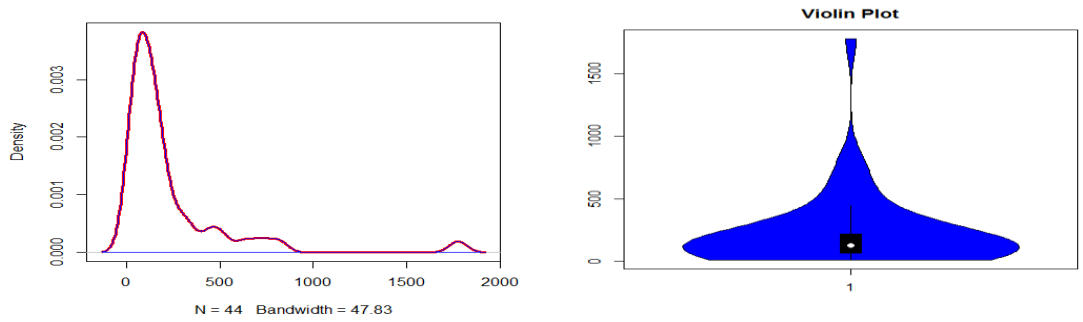

Figure 13: The III data set's violin plot and kernel density.

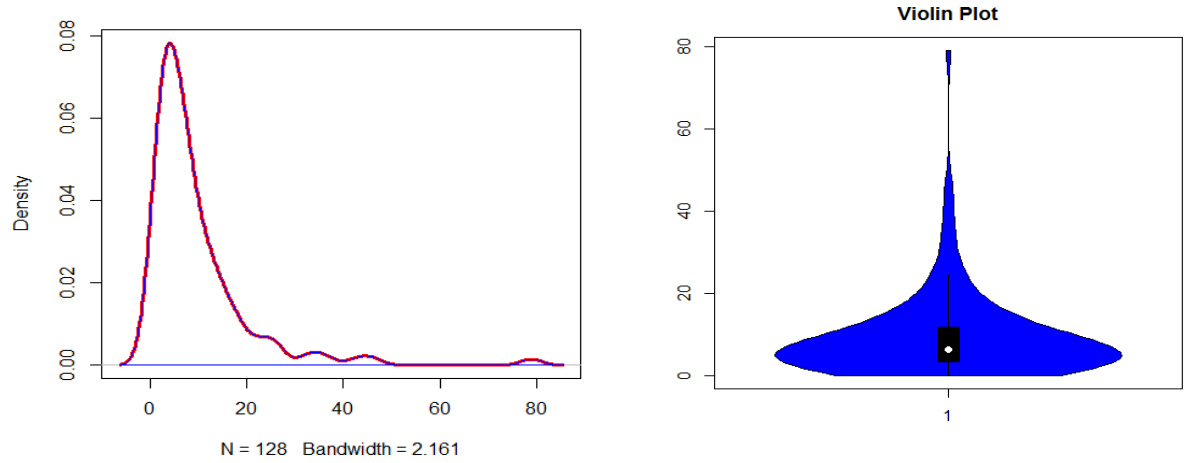

Figure 14: The IV data set's violin plot and kernel density.

Figures 11, 12, 13 and 14 show the kernel density and violin plots for the first and second data sets. The kernel density plot depicts the distribution of the data, with smoother curves suggesting density, whereas the violin plot combines the density plot with box plot elements to provide insights into the distribution, spread, and central tendency.

Table 4: The failure time data set's descriptive statistics.

Data sets	n	Mini	Mean	Median	s.d	Skewness	kurtosis	Maxi	Range	S.E
I	21	17.88	73.56	67.8	39.06	0.79	-0.07	174.4	156.52	8.52
II	72	0.10	1.77	1.50	1.03	1.31	1.85	5.55	5.45	0.12
III	44	12.2	223.48	128.5	305.43	3.27	12.82	1776	1763.8	46.05
IV	128	0.08	9.37	6.39	0.51	3.25	15.2	79.05	78.97	0.93

The kurtosis of Dataset I is similar to that of a normal distribution, and it exhibits significant right skewness and somewhat high variability. Dataset II has a moderate dispersion and is right-skewed with a few outliers. The data is properly represented by the mean. Large outliers may be present in Dataset III due to its severe right skewness and thick tails. Extreme kurtosis and considerable right skewness are shown in Dataset IV. The data distribution is highly tailed, indicating the presence of numerous outliers despite the huge sample size shown in Table 4.

Table 5 MLEs, standard errors, confidence intervals in parentheses, values for the failure time data set I.

Models	$\hat{c}$	$\hat{k}$	$\hat{\theta}$	$\hat{\alpha}$	$\hat{\beta}$
NEBIII	0.3498 (0.6494)	4.3762 (0.8775)	5.7008 (2.0085)	-	-
BIII	1.2226 (0.1342)	111.7730 (4.5719)	-	-	-
BXII	8.8716 (4.5920)	0.0271 (0.1360)	-	-	-
EBXII	2.4900 (5.3806)	0.5488 (5.5972)	-	201.9686 (1.0991)	-
OBIIILx	35.2764 (2.8729)	0.1020 (0.1600)	0.1723 (0.0510)	2.3352 (2.3719)	-

Table 5 and 7 shows that the model parameter's MLEs for the failure time data set I are displayed in the table together with the standard errors and 95% confidence intervals (in parentheses). The standard errors show how accurate the estimates are, while these estimates shed light on the data's underlying distributional features. Confidence intervals provide a measure of

statistical reliability and model resilience by further quantifying the range that the genuine parameter values are likely to fall inside.

Table 6 Failure time data set I log-likelihood, AIC, BIC, CAIC, HQIC, A, W, and KS (p-value) values.

Models	W	A	KS (p-value)	AIC	BIC	CAIC	HQIC
NEBIII	0.0641	0.4808	0.1225 (0.9110)	218.9961	222.1296	220.4078	219.6761
BIII	0.0860	0.3518	0.2085 (0.3205)	222.4910	224.5801	223.1577	222.9444
BXII	0.2318	0.0311	0.5071 (0.00004)	280.5735	282.6625	281.2402	281.0269
EBXII	0.0523	0.3984	0.1861 (0.4607)	221.9361	225.0696	223.3478	222.6161
OBIIILx	0.0878	0.5338	0.1691 (0.5849)	220.0265	224.2046	222.5265	220.9332

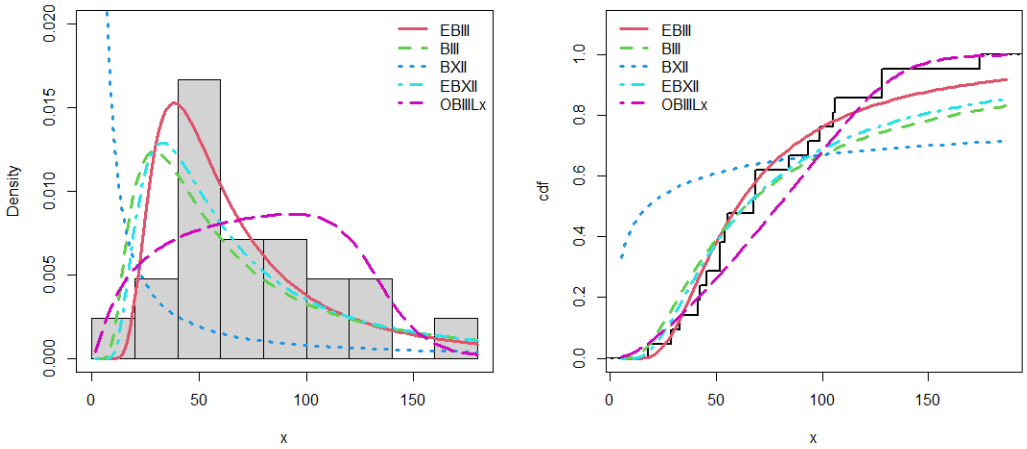

Figure 15: The plots for the estimated pdf and cdf of the EBII, BIII, BXII, EBX11, OB111Lx model for I data set.

Figure 15 illustrates the density plots and cumulative distribution functions (CDFs) of various distributions for data I. The density plot of NEBIII exhibits a right-skewed distribution, while BIII also shows a right-skewed distribution. BXII has a decreasing density, and EBXII displays a right-skewed pattern as well. In contrast, the OBIIILx distribution has a symmetric density. The CDFs of all the distributions are non-decreasing.

Figure 16 presents the density plots of the same distributions for data 2, with notable differences. NEBIII, BIII, BXII, and EBXII all display right-skewed densities. Meanwhile, the OBIIILx distribution shows a decreasing density. All distributions have non-decreasing cdfs.

Table 7 MLE, standard error, and confidence interval values for the second failure time data set are enclosed in parenthesis.

Models	$\hat{c}$	$\hat{k}$	$\hat{\theta}$	$\hat{\alpha}$	$\hat{\beta}$
NEBIII	7.1838(2.9106)	5.9956(4.7896)	0.3516(0.1331)	-	-
BIII	2.2340(0.2152)	1.9165(0.2259)	-	-	-
BXII	2.4447(0.9026)	0.9388(0.4849)	1.8038(0.9034)	-	-
EBXII	3.8131(0.5440)	0.4783(0.0792)	-	-	-
OBIIILx	37.4049(3.3352)	0.0289(0.2091)	0.6203(0.0123)	2.2476(0.0052)	-

Table 8: KS (P-values) for failure time data set II includes log-likelihood, AIC, BIC, CAIC, HQIC, A, W, and KS.

Models	A	W	KS(P-value)	AIC	BIC	CAIC	HQIC
NEBIII	0.3543	0.0618	0.0679(0.8936)	191.2533	198.0833	191.6063	193.9724
BIII	0.7632	0.1002	0.1121(0.3259)	199.0102	203.5635	199.1841	200.8229
BXII	0.7647	0.1003	0.11164(0.3308)	200.9952	207.8252	201.3481	203.7142
EBXII	0.8993	0.1193	0.1294(0.1793)	200.8386	205.392	201.0125	202.6513
OBIIILx	2.4706	0.4217	0.2326	226.9613	236.0680	227.5584	230.5867

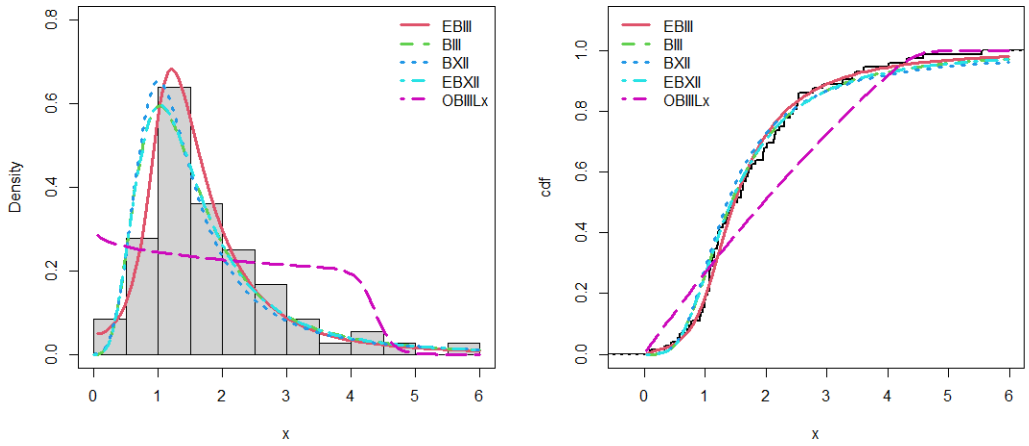

Figure 16: The plots for the estimated pdf and cdf of the EBII, BIII, BXII, EBX11, OB111Lx model for II data set.

Table 9: KS (p-value), AIC, BIC, CAIC, HQIC, and MLEs values head and neck cancer data set III.

Models	KS p-value	AIC	CAIC	BIC	HQIC	MLEs
NEBIII	0.8273	564.8779	565.4779	570.2304	566.8629	0.8909764 48.3109586 1.1537476
EBXII	0.55	570	571	575	572	2.2172245 0.3520043 27.2185919
NEW	0.5573	832	832	837	834	0.09390543 1.04777286
W	0.3242	567	567	571	569	0.006412296 0.939411119
NB	6.864e-09	657	657	660	658	4.766857500. 04328101
OBIIILx	0.013	583	584	590	586	10.60543426 0.994406630. 07977207 0.02078850

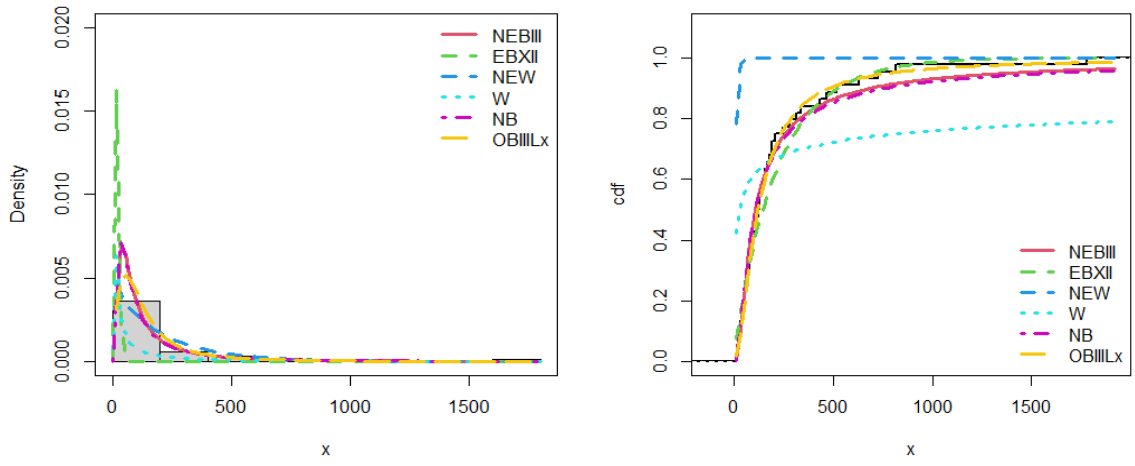

Figure 17: The plots for the estimated pdf and cdf of the NEBIII, EBXII, NEW, W, NB, OB111Lx model for III data set.

Figure 17 shows the density plots of the same distributions for data 3, with some significant variations. The densities of NEBIII, NEW, W, NB and OBIIILx are all right-skewed. Meanwhile, a decreasing density is seen in the EBXII distribution. CDFs are non-decreasing for all distributions.

Table 10 Log-likelihood, A, W and KS (*p*-value), AIC, BIC, CAIC, and HQIC 128 bladder cancer patient's values for failure time data set IV.

Models	**W**	**A**	**KS (P-value)**	**AIC**	**CAIC**	**BIC**	**HQIC**	**MLE**
NEBIII	0.3421	2.1886	0.0957 (0.1912)	852.9925	853.186	861.5486	856.4688	2.9276760 45.4766655 0.3475645
EBXII	0.3448703	2.190692	0.098282 (0.1686)	855.5293	855.7229	864.0854	859.0057	0.6538326 1.9008361 9.2510763
BIII	0.3856	2.454323	0.10173 (0.1413)	857.3729	857.4689	863.0769	859.6905	1.033300 4.207026
NB	0.7497285	4.554885	0.25067 (2.066e-07)	911.0332	911.1292	916.7372	913.3508	2.3348084 0.2337527
OBIIILx	0.6241582	3.754344	0.18126 (0.0004447)	878.0501	878.3753	889.4582	882.6853	35.68090326 0.03293536 0.19766194 1.04961243

By showing lower values for statistical metrics like the W-statistic, A, AIC, CAIC, BIC, and HQIC, Tables 6, 8, 9, and 10 show that the NEBIII model consistently performs better than its rival models. Furthermore, when compared to its alternatives, the NEBIII model produces higher p-values, indicating a better fit to the data.

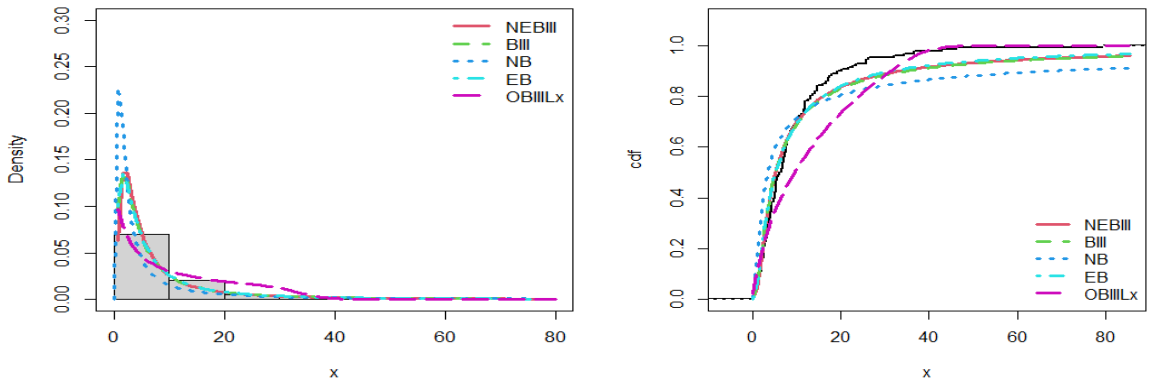

Figure 18: The plots for the estimated pdf and cdf of the NEBIII, BIII, EBXII, NB, OBIIILx model for IV data set.

Figure 18 shows the density plots of the same distributions for data 4, with some significant variations. NB, EBXII, BIII, and NEBIII are all skewed to the right. In the meantime, the OBIIILx distribution shows a declining density. All distributions have non-decreasing CDFs.

9.2 Applications of the MEBE distribution

This section presents the MEBE model's analysis of a real data set and compares it to the other fitted models. We use data dataset I gave in section 7.1 for comparison purposes. Secondly, we consider another data set named data set V, which is not used in section 7.1. The supplied information in data set V on servicing durations (in 1000 hours) for a particular windshield model by [25].

Table 11: For data set I, MLE's, standard errors in parenthesis, A, W, and KS (p-value) are shown as.

Models	$\hat{c}$	$\hat{k}$	$\hat{\theta}$	$\hat{u}$	$\hat{p}$	A	W	KS (p-value)
MEBE	0.4129 (0.6874)	5.7079 (4.3992)	6.3093 (1.8876)	0.0166 (0.0132)	0.8409 (0.1754)	0.2500	0.0371	0.0952 (0.9911)
E	-	-	-	0.0136 (0.0029)	-	0.1795	0.0307	0.2886 (0.0603)

EBIII	0.3483 (0.6448)	4.3527 (1.7494)	5.7292 (2.0359)	-	-	0.4807	0.0641	0.1224 (0.9111)

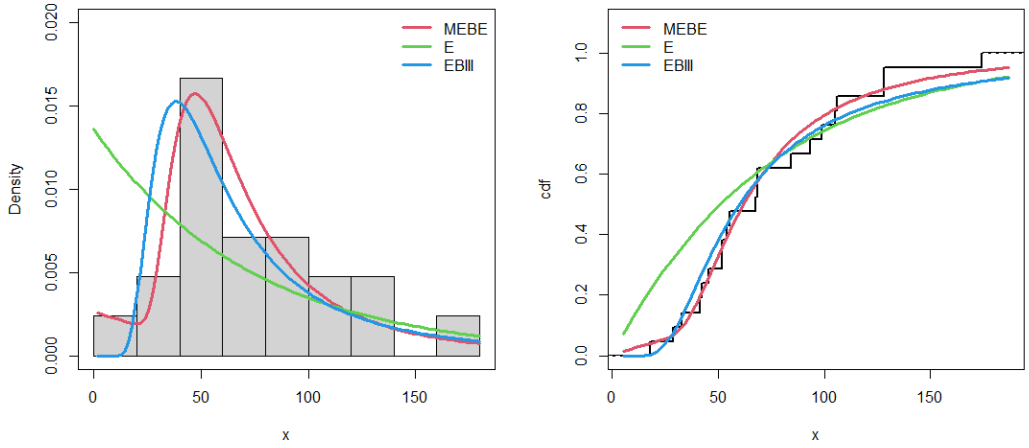

Figure 19: The estimated PDF of MEBE for several parametric values for data set I.

A right-skewed distribution in MEBE and EBIII while the distribution E shows a decreasing trend, and the CDF plots show a non-decreasing pattern shown in Figure 19.

Table 12: KS (p-value), A, W, and MLEs (standard errors in parenthesis) for data set V.

Models	$\hat{c}$	$\hat{k}$	$\hat{\theta}$	$\hat{u}$	$\hat{p}$	A	W	KS (p-value)
MEBE	1.5981 (1.5745)	3.2278 (2.8843)	1.7707 (1.9330)	0.7173 (0.2992)	0.6259 (0.1692)	0.5916	0.1084	0.1692 (0.4495)
E	0.4795 (0.0604)	-	-	-	-	1.1264	0.1861	0.2078 (0.0072)
EBIII	5.6175 (2.3411)	6.1610 (5.7751)	0.3179 (0.1178)	-	-	1.7688	0.3001	0.1606 (0.0689)

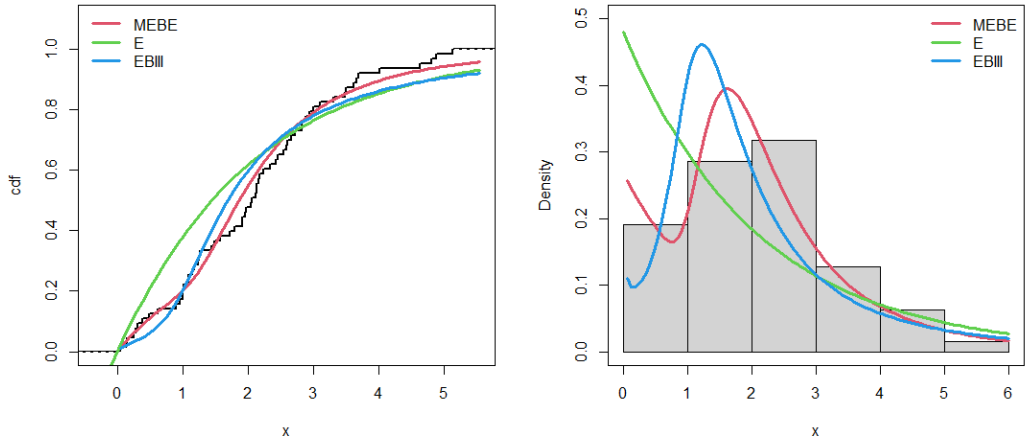

Figure 20: The estimated PDF and CDF of MEBE for several parametric values for data set V.

Density plots and cdf of various distributions are displayed in Figure 20. All distributions have non-decreasing cdf, while MEBE, E, and EBIII exhibit right-skewed, right-skewed, and decreasing behavior, respectively.

The MEBE model outperforms its competitors, as demonstrated by Tables 11 and 12, which display lower values for statistical metrics such as the W-statistic, A, AIC, CAIC, BIC, and HQIC. Additionally, the MEBE model yields higher p-values than its alternatives, suggesting a better fit to the data.

10. Conclusion

In this article, we introduce the New Extended Burr–III (NEB-III) distribution, a novel extension of the Burr–III distribution that provides enhanced flexibility and accuracy for modeling real-world data. We also derive the mixture model of the Mixture Extended Burr and Exponential (MEBE) distribution and present it. For the MEBE distribution, we give an analytical treatment of the density and hazard rate functions. The subsection illustrates the importance of the NEBIII distribution with four real-data applications. The NEBIII distribution provides a superior fit than comparison models like EBXII, OBIIIILx, BIII, BXII, NB, NEW, and W, as shown in Tables 6, 8, 9, and 10. Figures 15, 16, 17, and 18 further support this finding. Tables 11–12 demonstrate that the mixture model performs better than its competitors. Figures 19 and 20 display the estimated PDF and CDF for the MEBE distribution with different parameter values for data sets I and V, respectively. The MEBE model offers a better fit than the other models, as the figures further demonstrate.

References

[1] S. Nasiru, P. N. Mwita, and O. Ngesa, "Exponentiated gen- eralized power series family of distributions," Annals of Data Science, vol. 6, no. 3, pp. 463–489, 2019.

[2] Y. L. Tung, Z. Ahmad, O. Kharazmi, C. B. Ampadu, E. H. Hafez, and S. A. Mubarak, "On a new modification of the Weibull model with classical and Bayesian analysis," Com- plexity, vol. 2021, Article ID 5574112, 19 pages, 2021.

[3] O. S. Balogun, M. Z. Iqbal, M. Z. Arshad, A. Z. Afify, and P. E. Oguntunde, "A new generalization of Lehmann type-II distribution: theory, simulation, and applications to survival and failure rate data," Scientific African, vol. 12, e00790, 2021.

[4] Lehmann, E.L. The power of rank tests. Ann. Math. Stat. 1952, 24, 23–43

[5] Murthy, D. N. P. and Jiang R. (1998) Mixture of Weibull distribution parameter characterization of failure date function, pp 47-65, John Wiley and Sons. Ltd

[6] Sultan. K.S, M.A. Ismail, A.S. Al-Moisheer (2006) Mixture of two inverse Weibull distributions Properties and estimation, Comp. Stat. Data Ana. 51, 5377 - 5387.

[7] Kareema Abulkadhum Makhrib (2012) On finite mixture of inverse Weibull distribution, Proc. ICCS- 12, Doha Qatar December 19-22, 2012, Vol.23, 53-60.

[8] Handique, L., Usman, R. M., & Chakraborty, S. (2020). New Extended Burr-III Distribution: Its Properties and Applications. *Thailand Statistician*, *18*(3), 267-280.

[9] Yang, H., Huang, M., Chen, X., He, Z., & Pu, S. (2024). Enhanced real-life data modeling with the modified Burr III odds ratio–G distribution. *Axioms*, *13*(6), 401.

[10] Jamal, F., Nasir, M. A., Tahir, M. H., & Montazeri, N. H. (2017). The odd Burr-III family of distributions. *Journal of Statistics Applications and Probability*, *6*(1), 105-122.

[11] Nkomo, W., Oluyede, B., & Chipepa, F. (2024). The new odd Burr III-G power series class of distributions: properties and applications to censored and uncensored data. *International Journal of Mathematical Modelling and Numerical Optimisation*, *14*(3-4), 109-140.

[12] Deepthy, G. S., Sebastian, N., & Chandra, N. (2023). Applications of Burr III-Weibull quantile function in reliability analysis. *Statistical Theory and Related Fields*, *7*(4), 296-308.

[13] Noori, N., & Khaleel, M. (2025). The Modified Burr-III Distribution Properties, Estimation, Simulation, with Application on Real Data. *Iraqi Statisticians journal*, *2*(special issue for ICSA2025), 225-246.

[14] Burr IW (1942) Cumulative frequency functions. Ann Math Stat 13(2):215–232.

[15] Muhammad, M., & Liu, L. (2022). A new extension of the beta generator of distributions. Mathematica Slovaca, 72(5), 1319–1336.

[16] Muhammad, M., Liu, L., Abba, B., Muhammad, I., Bouchane, M., Zhang, H., et al. (2023). A new extension of the Topp–Leone-family of models with applications to real data. Annals of Data Science, 10(1), 225–250.

[17] Abbas, S., Muhammad, M., Jamal, F., Chesneau, C., Muhammad, I., & Bouchane, M. (2023). A new extension of the Kumaraswamy generated family of distributions with applications to real data. Computation, 11(2), 26.

[18] Lorenz, M. O. (1905). Methods of measuring the concentration of wealth. Publications of the American statistical association, *9*(70), 209-219.

[19] Bonferroni C.E. (1930). Elmenti di statistica generale. Libreria Seber, Firenze.

[20] Zenga M.(1984). Argomenti di Statistica, Vita e Pensiero, Milano Methods of measuring the concentration of wealth. Publications of the American statistical association, 9(70), 209-219.

[21] Pietra, G. (1915). Delle relazioni tra gli indici di variabilitā. C. Ferrari.

[22] Barter, H. L. (1988). History and role of order statistics. Communications in Statistics. Theory and Methods, 17(7), 2091–2107.

[23] Shrahili, M., & Kayid, M. (2023). Excess lifetime extropy of order statistics. Axioms, 12(11), 1024

[24] Artzner, P., Delbaen, F., Eber, J. M., & Heath, D. (1999). Coherent measures of risk. Mathematical Finance, 9(3), 203–228.

[25] Murthy, D.N.P., Xie, M. and Jiang, R. (2004) Weibull Models. John Wiley & Sons, New York.

Declaration

Conflict of Study: The author declares that he has no known competing financial interests or personal relationships that could have appeared to influence the work reported in this paper

Author Contribution Statement: All auhors conceived the idea and designed the research; Analyzed and interpreted the data, and wrote the paper.
Funding Statement: This research did not receive any specific grant from funding agencies in the public, commercial, or not-for-profit sectors.
Availability of Data and Material: Data will be made available by the corresponding author on reasonable request.
Consent to Publish: All authors have agreed to publish this manuscript in the SCOPUA Journal of Applied Statistical Research (JASR)- ISSN(e): 3104-4794.
Ethical Approval: Not Applicable
Consent to Participate: Not Applicable
Acknowledgment: Not Applicable.

Authors' Note

Manahil Fatima: manahilf6551@gmail.com

Muzna Sarwar: muznastatphd@gmail.com

Shoaib Iqbal: shoaibiqbalqau654@gmail.com

Zawar Hussain: zhlangah@yahoo.com

Farrukh Jamal: fshakir@ut.edu.sa